JCTC Journal of Chemical Theory and Computation

pubs.acs.org/JCTC Article

Accelerating Excitation Energy Computation in Molecules and Solids within Linear-Response Time-Dependent Density Functional Theory via Interpolative Separable Density Fitting Decomposition

Wei Hu, Jie Liu,* Yingzhou Li, Zijing Ding, Chao Yang, and Jinlong Yang*

Cite This: J. Chem. Theory Comput. 2020, 16, 964−973

Read Online

ACCESS | Metrics & More | Article Recommendations | Supporting Information

ABSTRACT: We present an efficient way to compute the excitation energies in molecules and solids within linear-response time-dependent density functional theory (LR-TDDFT). Conventional methods to construct and diagonalize the LR-TDDFT Hamiltonian require ultrahigh computational cost, limiting its optoelectronic applications to small systems. Our new method is based on the interpolative separable density fitting (ISDF) decomposition combined with implicitly constructing and iteratively diagonalizing the LR-TDDFT Hamiltonian and only requires low computational cost to accelerate the LR-TDDFT calculations in the plane-wave basis sets under the periodic boundary condition. We show that this method accurately reproduces excitation energies in a fullerene (C_{60}) molecule and bulk silicon Si_{64} system with significantly reduced computational cost compared to conventional direct and iterative calculations. The efficiency of this ISDF method enables us to investigate the excited-state properties of liquid water absorption on MoS_2 and phosphorene by using the LR-TDDFT calculations. Our computational results show that an aqueous environment has a weak effect on low excitation energies but a strong effect on high excitation energies of 2D semiconductors for photocatalytic water splitting.

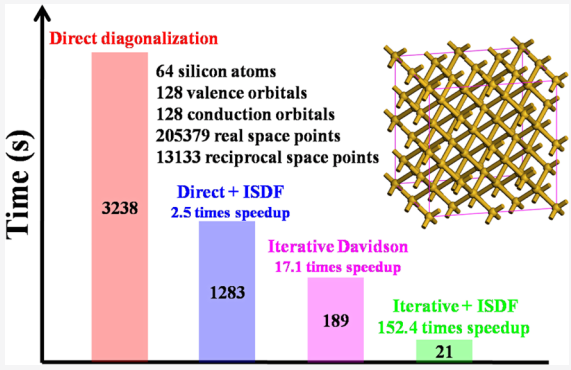

1. INTRODUCTION

Time-dependent density functional theory (TDDFT)[1] is a powerful tool to describe the excited-state properties in molecules and solids, which are essential to understanding photochemical phenomena, such as photocatalysis and photovoltaics. There are two schemes for solving the time-dependent Schrödinger equation within the framework of TDDFT.[2,3] One is to propagate the molecular orbitals on a real-space grid in the time domain following a transient photoexcitation,[4] known as real-time TDDFT (RT-TDDFT), which is particularly suitable for the study of electron dynamics. Another is the Casida[5] or Sternheimer[6] equation formulated in the frequency domain via linear-response theory, also known as linear-response TDDFT (LR-TDDFT), which is the most common formulation used to simulate excited-state properties, such as excitation energies and absorption spectra. The excited-state simulations by using the RT-TDDFT or LR-TDDFT schemes have been reported for a large variety of photoinduced processes in molecular and solid materials. However, as the system size increases, the cost of conventional LR-TDDFT calculations becomes prohibitively expensive.[2,3] Therefore, it is still challenging to explore the excited-state properties of large-scale systems containing hundreds of atoms with the LR-TDDFT calculations.

For small molecular systems, the LR-TDDFT calculations can be directly solved by using the direct diagonalization method. For this method, there are two expensive parts: one is to explicitly construct the LR-TDDFT Hamiltonian with high computational complexity of $O(N_e^5)$, and another is to directly diagonalize the LR-TDDFT Hamiltonian with ultrahigh computational complexity of $O(N_e^6)$ where N_e is the number of electrons in the systems. This method has been widely used in small localized basis sets, especially for Gaussian basis sets. However, for large molecular and solid systems, the direct diagonalization method becomes prohibitively expensive as the system size increases, especially for large uniform basis sets with high accuracy, such as the plane-wave basis sets.

An alternative more effective method to extract low-lying excited-state energies by using implicitly constructing and iteratively diagonalizing the LR-TDDFT Hamiltonian is the subspace iterative diagonalization method, such as the Davidson,[7] Lanczos,[8] and LOBPCG[9] algorithms. The iterative diagonalization method only requires low computational

Received: October 11, 2019
Published: January 3, 2020

Downloaded via DUKE UNIV on February 14, 2020 at 22:08:33 (UTC).
See https://pubs.acs.org/sharingguidelines for options on how to legitimately share published articles.

ACS Publications © 2020 American Chemical Society

https://dx.doi.org/10.1021/acs.jctc.9b01019
J. Chem. Theory Comput. 2020, 16, 964−973

complexity of $O(N_e^3) \sim O(N_e^4)$ and can be used in both small localized (Gaussian) and large uniform (plane-wave) basis sets.[10,11]

For the construction of the LR-TDDFT Hamiltonian, various methods have also been proposed for improving the efficiency of computing the two-electron integrals, such as the Resolution-of-the-identity (RI-K)[12−15] approximation, pair-atomic resolution-of-identity (PARI-K)[16] method, the occupied orbital RI-K (occ-RI-K)[17] algorithm, the chain-of-spheres exchange (COSX)[18,19] algorithm, the auxiliary density matrix method (ADMM),[20,21] and the tensor hypercontraction (THC) method.[22,23] In particular, Rappoport and Furche have introduced the RI approximation[24] to speed up the LR-TDDFT calculations of excitation energies and analytical gradients with local exchange-correlation functionals, such as local-density approximation (LDA)[25] and generalized gradient approximation (GGA).[26]

The recently developed interpolative separable density fitting (ISDF) decomposition[27] is able to efficiently compress the redundant information in the set of orbital pairs and is suitable for speeding up the two-electron integrals as well. The key step of the ISDF decomposition is to select a set of nonuniform grid points so that the values of the orbital pairs evaluated at such grid points can be used to accurately interpolate those evaluated at all grid points. The ISDF method is similar in spirit to the THC approach.[22,23] The ISDF method has so far been applied to two-electrons integrals,[27] random phase approximation,[28] density functional perturbation theory,[29] hybrid density functionals,[30−32] Bethe−Salpeter equation,[33] quantum Monte Carlo simulations,[34] and Møller−Plesset perturbation theory.[35] It should be noted that this ISDF method can be used in both the atomic orbital and canonical molecular orbital representation without knowing in advance the form of auxiliary basis functions. For this reason, the ISDF method can be used in both plane-wave[30] and Gaussian[34,35] basis sets.

In the present work, we present an efficient approach to reduce the computational cost of LR-TDDFT calculations by combining the ISDF decomposition with the iterative diagonalization method. Our approach is to construct low-rank decomposition to the Hartree-exchange-correlation integrals associated with the LR-TDDFT Hamiltonian and to iteratively diagonalize the LR-TDDFT Hamiltonian. This approach reduces the complexity of the LR-TDDFT Hamiltonian construction to $O(N_e^3)$ with a much small pre-constant. Here, we implement this ISDF decomposition for accelerating the LR-TDDFT calculations in the KSSOLV[36] software package, which is a MATLAB toolbox for solving the Kohn−Sham equations in the plane-wave basis sets under the periodic boundary condition. We show that this novel approach accurately reproduces excitation energies in molecules and solids with a significantly reduced computational cost. We use the LR-TDDFT + ISDF calculations to investigate the excited-state properties of liquid water absorption on MoS_2 and phosphorene.

This paper is organized as follows. Section 2 gives a brief description of the theoretical methodology, covering the LR-TDDFT method, the ISDF method, the combination of the LR-TDDFT and ISDF methods, and then the iterative ISDF method. Section 3 validates the computational accuracy and efficiency of the ISDF decomposition to accelerate the LR-TDDFT calculations and then presents scientific applications to liquid water on 2D semiconductors. A summary and outlook is given in Section 4.

2. METHODOLOGY

2.1. Linear-Response Time-Dependent Density Functional Theory. The linear-response time-dependent density functional theory (LR-TDDFT) yields an eigenvalue problem of the form

$$HX = \Lambda X \tag{1}$$

where X is the excitation wavefunctions and Λ is the corresponding excitation energies. The LR-TDDFT Hamiltonian H has the following block structure

$$H = \begin{bmatrix} D + 2V_{\mathrm{Hxc}} & 2W_{\mathrm{Hxc}} \\ -2W_{\mathrm{Hxc}}^{\dagger} & -D - 2V_{\mathrm{Hxc}}^{\dagger} \end{bmatrix} \tag{2}$$

where $D(i_v i_c, j_v j_c) = (\epsilon_{i_c} - \epsilon_{i_v})\delta_{i_v j_v}\delta_{i_c j_c}$ is an $N_{vc} \times N_{vc}$ ($N_{vc} = N_v N_c$) diagonal matrix with the orbital energies ϵ_{i_v} ($i_v = 1,2, ..., N_v$) associated with selected valence orbitals $\psi_{i_v}(\mathbf{r})$ and the orbital energies ϵ_{i_c} ($i_c = 1,2, ..., N_c$) associated with selected conduction orbitals $\psi_{i_c}(\mathbf{r})$ used in the LR-TDDFT calculations. These energies are typically obtained from the Kohn−Sham density functional theory (KSDFT) calculations. The V and W matrices represent the Hartree-exchange-correlation integrals defined as

$$\begin{aligned} V_{\mathrm{Hxc}}(i_v i_c, j_v j_c) &= \int \psi_{i_v}^*(\mathbf{r})\psi_{i_c}(\mathbf{r}) f_{\mathrm{Hxc}}(\mathbf{r}, \mathbf{r}')\psi_{j_v}(\mathbf{r}')\psi_{j_c}^*(\mathbf{r}') \, d\mathbf{r}\, d\mathbf{r}' \\ W_{\mathrm{Hxc}}(i_v i_c, j_v j_c) &= \int \psi_{i_v}^*(\mathbf{r})\psi_{i_c}(\mathbf{r}) f_{\mathrm{Hxc}}(\mathbf{r}, \mathbf{r}')\psi_{j_v}^*(\mathbf{r}')\psi_{j_c}(\mathbf{r}') \, d\mathbf{r}\, d\mathbf{r}' \end{aligned} \tag{3}$$

where f_{Hxc} is the Hartree-exchange-correlation kernel defined as

$$\begin{aligned} f_{\mathrm{Hxc}}(\mathbf{r}, \mathbf{r}') &= \nu_{\mathrm{H}}(\mathbf{r}, \mathbf{r}') + f_{\mathrm{xc}}[\rho](\mathbf{r}, \mathbf{r}') \\ &= \frac{1}{|\mathbf{r} - \mathbf{r}'|} + \frac{\delta \nu_{\mathrm{xc}}[\rho](\mathbf{r})}{\delta \rho(\mathbf{r}')} \end{aligned} \tag{4}$$

where $\rho(\mathbf{r}) = \Sigma_{i_v}^{N_e} |\psi_{i_v}(\mathbf{r})|^2$ is the electron density.

Under the Tamm−Dancoff approximation (TDA),[3] W_{Hxc} can be neglected and H becomes the Hermitian matrix rewritten as

$$H = D + 2V_{\mathrm{Hxc}} \tag{5}$$

where the Hartree-exchange-correlation integrals V_{Hxc} can be rewritten as the multiplication of $f_{\mathrm{Hxc}} \in \mathbb{C}^{N_r \times N_r}$ with the transposed Khatri−Rao product (also known as face-splitting product)[37] matrix $P_{vc} = \{\rho_{vc}(\mathbf{r}) := \psi_{i_v}^*(\mathbf{r})\psi_{i_c}(\mathbf{r})\} \in \mathbb{C}^{N_r \times N_{vc}}$ for the valence and conduction orbitals ($\psi_{i_v}(\mathbf{r})$ and $\psi_{i_c}(\mathbf{r})$) in real space ($\{\mathbf{r}_i\}_{i=1}^{N_r}$)

$$\begin{aligned} V_{\mathrm{Hxc}} &= P_{vc}^{\dagger} f_{\mathrm{Hxc}} P_{vc} \\ &= P_{vc}^{\dagger} \nu_{\mathrm{H}} P_{vc} + P_{vc}^{\dagger} f_{\mathrm{xc}} P_{vc} \end{aligned} \tag{6}$$

For simplicity, we only use the local-density approximation (LDA) functional in the KSDFT calculations in this work.

https://dx.doi.org/10.1021/acs.jctc.9b01019
J. Chem. Theory Comput. 2020, 16, 964−973

Because the LDA exchange-correlation kernel f_{xc} is diagonal in real space ($\{\mathbf{r}_i\}_{i=1}^{N_r}$), the exchange-correlation integral $V_{xc} = P_{vc}^{\dagger} f_{xc} P_{vc}$ can be directly and efficiently computed in real space but with a high computational complexity of $N_r N_v^2 N_c^2 \sim O(N_e^5)$. For the Hartree integral $V_H = P_{vc}^{\dagger} v_H P_{vc}$, we need to transform it into reciprocal space ($\{\mathbf{G}_i\}_{i=1}^{N_g}$), in which the Hartree potential v_H is diagonal $\hat{v}_H(\mathbf{G}) = 4\pi/|\mathbf{G}|^2$ (notice that $\hat{v}_H(\mathbf{G} = 0) = 0$) and the $V_H = \hat{P}_{vc}^{\dagger} \hat{v}_H \hat{P}_{vc}$ can be efficiently computed in reciprocal space. In this work, we use the fast Fourier transforms (FFTs) to transform between real ($\{\mathbf{r}_i\}_{i=1}^{N_r}$) and reciprocal ($\{\mathbf{G}_i\}_{i=1}^{N_g}$) spaces. In addition to performing $N_v N_c \sim O(N_e^2)$ FFTs to transfer from $P_{vc} = \{\rho_{vc}(\mathbf{r})\} \in \mathbb{C}^{N_r \times N_{vc}}$ to $\hat{P}_{vc} = \{\hat{\rho}_{vc}(\mathbf{G})\} \in \mathbb{C}^{N_g \times N_{vc}}$, the Hartree integral V_H still requires a high computational complexity of $N_g N_v^2 N_c^2 \sim O(N_e^5)$.

After constructing the LR-TDDFT Hamiltonian H, the next step is to explicitly diagonalize the LR-TDDFT Hamiltonian H with an ultrahigh complexity of $N_v^3 N_c^3 \sim O(N_e^6)$ and obtain the excitation wavefunctions X and energies Λ.

It should be noted that, for large uniform basis sets, such as plane-waves, N_g is typically much larger than N_v or N_c. The number N_o of occupied orbitals is either N_e or $N_e/2$ depending on how the spin is counted. The number of conduction orbitals N_c included in the LR-TDDFT calculations is typically a small multiple of N_v (the precise number being a free parameter to be converged), whereas N_g is often much larger than $100 \times N_e$ due to the high accuracy of plane-wave basis sets. In addition, the grid number in real space is typically 15 times larger than that in reciprocal space ($N_r \approx 15 \times N_g$) in the plane-wave basis sets.

2.2. Interpolative Separable Density Fitting Decomposition. In order to reduce the computational cost of two-electron integrals for constructing the LR-TDDFT Hamiltonian, one efficient way is to exploit the numerical rank deficiency of the pair products $\{\rho_{ij}(\mathbf{r}) := \psi_i(\mathbf{r})\phi_j(\mathbf{r})\}_{1 \le i \le m, 1 \le j \le n}$ of orbitals ($\psi_i(\mathbf{r})$ and $\phi_j(\mathbf{r})$) in real space by using the low-rank approximation. Several methods, including the Resolution-of-the-identity (RI-K)[12−15] approximation, the tensor hypercontraction (THC)[22,23] method, and the interpolative separable density fitting (ISDF) decomposition,[27,30,31] have been proposed to use a small number N_μ of auxiliary basis functions (ABFs) $\{\xi_\mu(\mathbf{r})\}_{1 \le \mu \le N_\mu}$ to represent $\rho_{ij}(\mathbf{r})$ so that

$$\rho_{ij}(\mathbf{r}) = \psi_i(\mathbf{r})\phi_j(\mathbf{r}) \approx \sum_{\mu=1}^{N_\mu} \xi_\mu(\mathbf{r}) C_\mu^{ij} \tag{7}$$

where C_μ^{ij} are the expansion coefficients (a third-order tensor). The key spirit of these methods lies in the fact that the orbital pair products $\{\rho_{ij}(\mathbf{r}) := \psi_i(\mathbf{r})\phi_j(\mathbf{r})\}_{1 \le i \le m, 1 \le j \le n}$ in real space are linearly dependent and the numerical rank deficiency can be revealed with the singular value decomposition (SVD).[38]

In particular, the key spirit of the ISDF decomposition is to decompose the third-order tensor $\{C_\mu^{ij}\}$ into a transposed Khatri−Rao product of two matrices

$$C_\mu^{ij} = \psi_i(\hat{\mathbf{r}}_\mu)\phi_j(\hat{\mathbf{r}}_\mu) \tag{8}$$

where $\{\hat{\mathbf{r}}_\mu\}_{\mu=1}^{N_\mu}$ denote a set of interpolation points, and then we have

$$\rho_{ij}(\mathbf{r}) = \psi_i(\mathbf{r})\phi_j(\mathbf{r}) \approx \sum_{\mu=1}^{N_\mu} \xi_\mu(\mathbf{r})\psi_i(\hat{\mathbf{r}}_\mu)\phi_j(\hat{\mathbf{r}}_\mu) \tag{9}$$

The interpolation points are selected from real space grid points $\{\mathbf{r}_i\}_{i=1}^{N_r}$ by using the randomized sampling QR factorization with column pivoting (QRCP)[30] procedure or machine learning methods (K-means clustering).[31] Both methods yield the smallest value $N_\mu \approx t\sqrt{mn}$ (where t is a small constant referred to as the rank parameter) superior to the RI-K and THC methods.[30] $\{\xi_\mu\}_{\mu=1}^{N_\mu}$ are the interpolation vectors (ABFs) sampled on real space $\{\mathbf{r}_i\}_{i=1}^{N_r}$, which can be efficiently computed with the least squares procedure. It should be noted that the computational complexity of the ISDF decomposition only scales as $O(N_e^3)$.[30]

Furthermore, the ISDF method can be applied in both plane-wave[30] and Gaussian[34,35] basis sets because it can be used in both the atomic orbital and canonical molecular orbital representations without knowing in advance the form of ABFs, superior to the RI-K and THC methods, which have been widely used in the Gaussian basis sets. For the Gaussian basis sets, the Head-Gordon group has recently done an interesting work to accelerate the Hartree−Fock and Møller−Plesset perturbation theory calculations by using the ISDF method.[35] In this work, we implement this ISDF decomposition for accelerating the LR-TDDFT calculations in the plane-wave basis sets under the periodic boundary condition.

In the context of LR-TDDFT, we have $m = N_v \sim O(N_e)$ and $n = N_c \sim O(N_e)$. Hence, the ISDF procedure can compress $mn \sim O(N_e^2)$ functions into a much smaller number ($N_\mu \approx tN_e \sim O(N_e)$) of ABFs $\{\xi_\mu(\mathbf{r})\}$. It should be noted that only this rank parameter t determines the computational accuracy of the ISDF method.

2.3. Low-Rank Representation for LR-TDDFT via ISDF. In the context of LR-TDDFT, the ISDF decomposition can be applied to the orbital product matrix $P_{vc} = \{\rho_{vc}(\mathbf{r}) := \psi_{i_v}^*(\mathbf{r})\psi_{i_c}(\mathbf{r})\} \in \mathbb{C}^{N_r \times N_{vc}}$ then

$$P_{vc} \approx \Xi(\Psi_v^* \odot \Psi_c) \tag{10}$$

where $\Xi = \{\xi_\mu(\mathbf{r})\}_{\mu=1}^{N_\mu} \in \mathbb{C}^{N_r \times N_\mu}$, $\Psi_v = \{\psi_{i_v}(\hat{\mathbf{r}}_\mu)\}_{\mu=1}^{N_\mu} \in \mathbb{C}^{N_\mu \times N_v}$, $\Psi_c = \{\psi_{i_c}(\hat{\mathbf{r}}_\mu)\}_{\mu=1}^{N_\mu} \in \mathbb{C}^{N_\mu \times N_c}$, and $\odot$ denotes the transposed Khatri−Rao product.

Under the ISDF decomposition of $P_{vc} = \{\rho_{vc}(\mathbf{r}) := \psi_{i_v}^*(\mathbf{r})\psi_{i_c}(\mathbf{r})\} \in \mathbb{C}^{N_r \times N_{vc}}$, the Hartree-exchange-correlation term can be written as

$$\begin{aligned} V_{Hxc} &= P_{vc}^{\dagger}(v_H + f_{xc})P_{vc} \\ &= (\Psi_v^* \odot \Psi_c)^*(\tilde{V}_H + \tilde{V}_{xc})(\Psi_v^* \odot \Psi_c) \end{aligned} \tag{11}$$

where $\tilde{V}_H = \Xi^{\dagger} v_H \Xi \in \mathbb{C}^{N_\mu \times N_\mu}$ and $\tilde{V}_{xc} = \Xi^{\dagger} f_{xc} \Xi \in \mathbb{C}^{N_\mu \times N_\mu}$ are the projected Hartree and exchange-correlation integrals under the auxiliary basis sets Ξ, respectively. Therefore, V_{Hxc} can be evaluated explicitly as three matrix multiplications performed in sequence, which is more efficient than conventional integrals with a high computational cost of $(N_g + N_r)N_v^2 N_c^2$. The computational cost of these calculations is significantly reduced to $(N_g + N_r)N_\mu^2 + N_\mu N_v^2 N_c^2$, where the first term is the cost of computing $\tilde{V}_H + \tilde{V}_{xc}$ under the ISDF basis set and the second term is the cost for three matrix multiplications. However, the computational complexity still highly scales up to $O(N_e^5)$, which is expensive even for systems containing hundreds of atoms. An effective solution is to combine implicitly constructing and iteratively diagonalizing the LR-TDDFT Hamiltonian, in which V_{Hxc} can be kept in the factored form

https://dx.doi.org/10.1021/acs.jctc.9b01019
J. Chem. Theory Comput. 2020, 16, 964−973

via ISDF. Then the computational cost bottleneck is only attributed to the first term of $(N_g + N_r)N_\mu^2 \sim O(N_e^3)$.

2.4. Iterative Diagonalization of LR-TDDFT via ISDF. In the conventional approaches, excitation energies and wavefunctions can be directly computed by explicitly diagonalizing the LR-TDDFT Hamiltonian H but with an ultrahigh complexity of $N_v^3N_c^3 \sim O(N_e^6)$. An improved approach is to use iterative diagonalization methods, such as the Davidson,[7] Lanczos,[8] and LOBPCG[9] algorithms, to implicitly diagonalize the LR-TDDFT Hamiltonian H with a moderate computational cost of $kN_v^2N_c^2 \sim kO(N_e^4)$ (k is the number of few desired eigenvalues and eigenvectors). Furthermore, if H is kept in the factored form, iterative diagonalization methods can further reduce the computational cost to $k(N_g + N_r)N_vN_c \sim kO(N_e^3)$. We use the Davidson method[10,11] recently developed in the LR-TDDFT calculations.

The Davidson method can iteratively solve the linear eigenvalue problem on a subspace $S_k \in \mathbb{C}^{N_{vc}\times k}$ with the form

$$HX_k = \Lambda_k X_k \tag{12}$$

The key step in the Davidson method is to project H onto the subspace S_k ($H_s = S_k^\dagger H S_k \in \mathbb{C}^{k\times k}$) and solve the projected eigenvalue problem $H_sC_k = S_k^\dagger S_k \Lambda_k C_k$. The excitation wavefunctions $X_k = S_kC_k$ can be directly computed from the subspace S_k and coefficients C_k.

It should be noted that $H_s = S_k^\dagger H S_k$ is required to compute from right-hand sides

$$H_s = S_k^\dagger D S_k + 2S_k^\dagger\{P_{vc}^\dagger[(\nu_H + f_{xc})(P_{vc}S_k)]\} \tag{13}$$

For each iteration in the Davidson method, the total computational cost of implicitly constructing and diagonalizing the LR-TDDFT Hamiltonian H is $k(N_g + N_r)N_vN_c + k^3 \sim kO(N_e^3)$ (Supporting Information). Therefore, this Davidson method can significantly reduce the total computational time in the LR-TDDFT calculations. The pseudocode of the Davidson method is shown in Algorithm 1.

Algorithm 1 Davidson method for solving the LR-TDDFT eigenvalue problem $Hx_i = \lambda_i x_i, i = 1, 2, \ldots, k$.

Input: Hamiltonian H and initial wavefunctions $\{x_i\}_{i=1}^k$.
Output: Eigenvalues $\{\lambda_i\}_{i=1}^k$ and wave functions $\{x_i\}_{i=1}^k$.

```
Initialize the trial subspace S_k = {s_i}_{i=1}^k and orthonormalize S_k.
while convergence not reached do
    Project H onto the subspace S_k: H_s ← S_k^† H S_k.
    Solve the projected eigenvalue problem H_s C_k = (S_k^† S_k) C_k Λ_k and obtain the coefficients
    C = {c_i}_{i=1}^k and eigenvalues Λ_k = {λ_i}_{i=1}^k.
    Compute X_k ← S_k C_k and the residual vectors R_k = H X_k − Λ_k X_k.
    Construct the subspace V with T R_k (where T is a preconditioner) and update the
    subspace S ← {S, V}.
end while
Update {x_i}_{i=1}^k ← X_k.
```

However, the standard Davidson method requires to implicitly constructing the LR-TDDFT Hamiltonian H during each iteration step with the computational cost of $k(N_g + N_r)N_vN_c$. For common molecular and solid systems, the standard Davidson method always takes several iterations (always larger than 10). Notice that for plane-wave basis sets, N_r and N_g are typically much larger than N_c or N_v ($N_r \approx 15 \times N_g$, $N_g \approx 100 \times N_v$, and $N_v \approx N_c$). Therefore, the standard Davidson method still takes much time for implicitly constructing the LR-TDDFT Hamiltonian H during each iteration step, although this iterative method is much faster than the direct diagonalization method, which requires explicitly constructing and directly diagonalizing the LR-TDDFT Hamiltonian.

Here, we propose to combine iterative methods with ISDF decomposition to further reduce the computational cost during each iteration step in the Davidson method. The key step is to project the Hartree-exchange-correlation term onto the ISDF subspace and obtain the projected H_{ISDF} under the ISDF ABFs Ξ, which is defined as

$$H_{ISDF} = (\Psi_v^\dagger \odot \Psi_c)^\dagger (D + 2\tilde{V}_H + 2\tilde{V}_{xc})(\Psi_v^\dagger \odot \Psi_c) \tag{14}$$

This expensive step only requires to one time constructing the projected H_{ISDF} with the computational cost of $k(N_g + N_r)N_\mu^2$.

For the iteration steps in the Davidson method, we only require to iteratively project the small Hamiltonian H_{ISDF} onto the subspace S_k with a cheap computational cost of $kN_\mu N_vN_c$ ($N_\mu \approx N_o$). Therefore, this Davidson + ISDF method can significantly reduce the total computational time compared to the standard Davidson method in the LR-TDDFT calculations.

For the Davidson + ISDF method, if the number of selected eigenvalues and eigenvectors is small ($k \ll N_e$), the complexity of diagonalizing the LR-TDDFT Hamiltonian only scales $O(N_e^3)$, similar to the case of implicitly constructing the LR-TDDFT Hamiltonian. The pseudocode of the Davidson + ISDF method is shown in Algorithm 2.

Algorithm 2 Davidson method for solving the LR-TDDFT eigenvalue problem $Hx_i = \lambda_i x_i, i = 1, 2, \ldots, k$ with the ISDF decomposition.

Input: Hamiltonian H and initial wavefunctions $\{x_i\}_{i=1}^k$.
Output: Eigenvalues $\{\lambda_i\}_{i=1}^k$ and wave functions $\{x_i\}_{i=1}^k$.

```
Apply the ISDF decomposition to the orbital products P_vc(r) ≈ Ξ(Ψ_v^† ⊙ Ψ_c).
Project the Hartree-exchange-correlation term on the ABFs Ξ and obtain the projected
H_ISDF = (Ψ_v^† ⊙ Ψ_c)^† (D + 2Ṽ_H + 2Ṽ_xc)(Ψ_v^† ⊙ Ψ_c) where Ṽ_H = Ξ^† v_H Ξ and Ṽ_xc = Ξ^† f_xc Ξ.
Initialize the trial subspace S_k = {s_i(N_vc)}_{i=1}^k and orthonormalize S.
while convergence not reached do
    Project H_ISDF onto the subspace S_k: H_s ← S_k^† H_ISDF S_k.
    Solve the projected eigenvalue problem H_s C_k = (S_k^† S_k) C_k Λ_k and obtain the coefficients
    C = {c_i}_{i=1}^k and eigenvalues Λ_k = {λ_i}_{i=1}^k.
    Compute X_k ← S_k C_k and the residual vectors R_k = H X_k − Λ_k X_k.
    Construct and the subspace V with T R_k (where T is a preconditioner) and update
    the subspace S ← {S, V}.
end while
Update {x_i}_{i=1}^k ← X_k.
```

Table 1 summarizes the computational cost for constructing (explicitly and implicitly) and diagonalizing (directly and iteratively) the LR-TDDFT Hamiltonian under the ISDF ABFs compared to conventional direct and iterative diagonalization methods in the LR-TDDFT calculations.

Table 1. Computational Cost for Constructing (Explicitly and Implicitly) and Diagonalizing (Directly and Iteratively) the LR-TDDFT Hamiltonian under the ISDF ABFs Compared to Conventional Methods in the LR-TDDFT Calculations[a]

LR-TDDFT	construction	diagonalization
direct	$(N_g + N_r)N_v^2N_c^2$	$N_v^3N_c^3$
direct + ISDF	$(N_g + N_r)N_\mu^2 + N_\mu N_v^2N_c^2$	$N_v^3N_c^3$
iterative	$k(N_g + N_r)N_vN_c$	$k(N_g + N_r)N_vN_c$
iterative + ISDF	$k(N_g + N_r)N_\mu^2$	$kN_\mu N_vN_c$

[a]Notice that $N_r \approx 15 \times N_g$, $N_g \approx 100 \times N_o$, and $N_\mu \approx N_v \approx N_c \approx N_o \sim O(N_e)$ in the plane-wave basis sets.

3. RESULTS AND DISCUSSION

In this section, we demonstrate the computational accuracy and efficiency of the ISDF decomposition to accelerate the LR-TDDFT calculations of excitation energies in molecules and solids. We implement the LR-TDDFT calculations in the

https://dx.doi.org/10.1021/acs.jctc.9b01019
J. Chem. Theory Comput. 2020, 16, 964−973

KSSOLV[36] software package, which is a MATLAB toolbox for solving the Kohn−Sham equations in the plane-wave basis sets under the periodic boundary condition. We use the Hartwigsen−Goedecker−Hutter (HGH) norm-conserving pseudopotentials[39] and the LDA[25] exchange-correlation functional in the LR-TDDFT calculations. All the calculations are sequentially carried out on a single core. We check the computational accuracy of these LR-TDDFT calculations[10,11] by comparing the results with those obtained from the standard pseudopotential plane-wave software Quantum ESPRESSO (QE).[40]

We perform the LR-TDDFT calculations for molecular and solid systems at the Γ point. In particular, we chose a fullerene (C_{60}) molecule and a bulk silicon Si_{64} system as plotted in Figure 1. All these systems are closed shell systems, and the

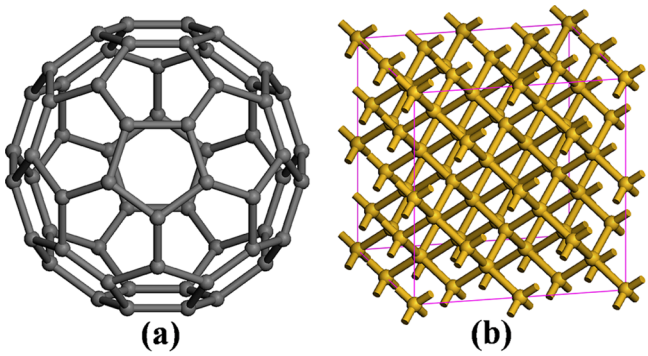

Figure 1. Atomic structures of (a) fullerene (C_{60}) molecule and (b) bulk silicon Si_{64} system. The gray and yellow balls denote carbon and silicon atoms, respectively.

number of occupied orbitals is $N_o = N_e/2$, where N_e is the valence electrons in the systems. In this work, we set the numbers of selected valence N_v and conduction N_c orbitals, the number k of selected excitation energies in iterative diagonalization methods in the LR-TDDFT calculations equal to the number N_o of occupied orbitals in the systems ($N_v = N_c = k = N_o$). The kinetic energy cutoff is set to 10 Ha for these two systems (Table 2).

Table 2. Computational Parameters of Fullerene (C_{60}) Molecule and Bulk Silicon Si_{64} System Used in the LR-TDDFT Calculations, Including the Supercell Length L (Bohr), the Grid Numbers N_r and N_g in Real and Reciprocal Space, and the Numbers N_v and N_c of Selected Valence and Conduction Orbitals

system	L	N_r	N_g	N_v	N_c
C_{60}	24.56	343000	22335	120	120
Si_{64}	20.53	205379	13133	128	128

3.1. Computational Accuracy of Excitation Energies. It should be noted that the computational accuracy of the ISDF decomposition to accelerate the LR-TDDFT calculations only depends the low-rank approximation of orbital product matrix P_{vc}. The rank value of N_μ used in the ISDF decomposition is the number of truncated singular values of P_{vc}, which can be directly computed by using the exact SVD method but with ultrahigh computational cost of $N_r^2N_vN_c + N_rN_v^2N_c^2 + N_v^3N_c^3 \sim O(N_e^6)$. Hererin, we can use the truncated singular values of P_{vc} to accurately estimate the rank value of N_μ in the LR-TDDFT + ISDF calculations.

Figure 2 plots the decremented singular values of orbital product matrix P_{vc} associated with the C_{60} molecule and bulk

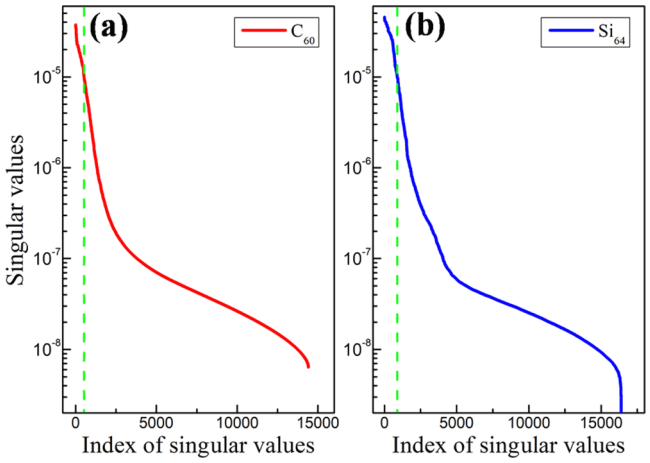

Figure 2. Decremented singular values of the orbital product matrix P_{vc} for (a) C_{60} ($N_v = N_c = N_o = 120$) and (b) Si_{64} ($N_v = N_c = N_o = 128$) systems computed with the exact SVD method.

silicon Si_{64} system. We find that the singular values of both C_{60} and Si_{64} decay rapidly with respect to the index of singular values increases. In particular, the leading 523 (out of 14400) and 886 (out of 16384) singular values for C_{60} and Si_{64} decrease rapidly toward zero (all other singular values are below 10^{-5}), respectively. The rank truncation ratios N_μ/N_{vc} are 0.036 and 0.054 (the corresponding rank parameters $t = N_\mu/N_v$ are 4.36 and 6.92) for C_{60} and Si_{64}, respectively. Therefore, the rank values of N_μ of C_{60} and Si_{64} are only roughly 0.05 out of full rank N_{vc} without sacrificing the accuracy of low-rank approximation of the orbital product matrix P_{vc}.

This prediction is confirmed in Figure 3, which shows the excitation energies and corresponding relative errors ($\Delta\Lambda = (\Lambda_{ISDF} - \Lambda)/\Lambda$, Λ_{ISDF}, and Λ are the excitation energies computed with and without the ISDF method, respectively) of C_{60} and Si_{64} systems computed with iterative Davidson and ISDF methods. Three rank truncation ratios $N_\mu/N_{vc} = 0.001$, 0.01, and 0.1 are used in these calculations, and corresponding rank parameters $t = N_\mu/N_v$ are 0.12, 1.2, and 12.0 for C_{60} and 0.128, 1.28, and 12.8 for Si_{64}. We find that, for both C_{60} and Si_{64} systems, the relative errors of excitation energies are negligible (below 10^{-4}) when the rank truncation ratio N_μ/N_{vc} is set to 0.1. Notice that these relative errors slowly increase as the rank truncation ratio is further decreased. The maximum relative errors are 0.001 and 0.002 when N_μ/N_{vc} are 0.01 and 0.001, respectively. It should be noted that the bulk Si_{64} system is more homogeneous than C_{60}; therefore, the computational accuracy of the Si_{64} system is higher than that of C_{60} by using the ISDF decomposition for the LR-TDDFT calculations.

3.2. Computational Efficiency. In this section, we demonstrate the computational efficiency of the ISDF decomposition to accelerate the LR-TDDFT calculations and report the computational cost for constructing (explicitly and implicitly) and diagonalizing (directly and iteratively) the LR-TDDFT Hamiltonian. The total time (in s) for the LR-TDDFT calculations with the ISDF decomposition is compared to conventional (direct and iterative) methods for

https://dx.doi.org/10.1021/acs.jctc.9b01019
J. Chem. Theory Comput. 2020, 16, 964−973

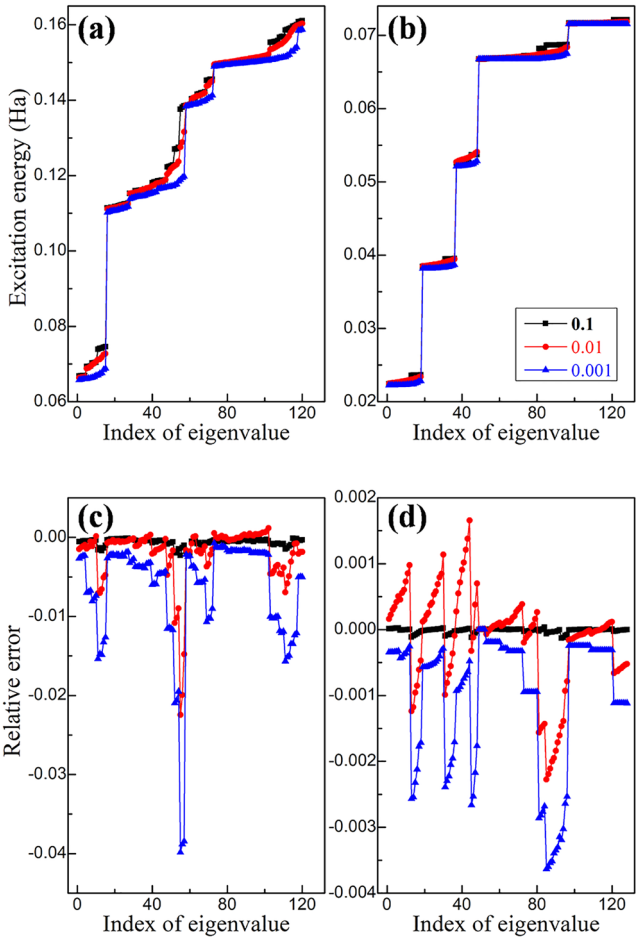

Figure 3. Excitation energies and corresponding relative errors of (a,c) C_{60} and (b,d) Si_{64} systems computed with iterative Davidson and ISDF methods. Three rank truncation ratios N_μ/N_{vc} = 0.001, 0.01, and 0.1 are used in the LR-TDDFT + ISDF calculations.

C_{60} and Si_{64} systems and summarized in Table 3. The total times of direct diagonalization in the LR-TDDFT calculations

Table 3. Total Time (in s) for the LR-TDDFT Calculations with the ISDF Decomposition Compared to Conventional (Direct and Iterative) Methods for C_{60} and Si_{64} Systems[a]

system	C_{60}	Si_{64}
direct diagonalization	2382.68	3238.45
direct + ISDF (0.1)	1123.06	1532.87
direct + ISDF (0.01)	843.05	1347.09
direct + ISDF (0.001)	832.46	1283.78
iterative Davidson	168.51	189.72
iterative + ISDF (0.1)	331.60	344.58
iterative + ISDF (0.01)	46.97	55.71
iterative + ISDF (0.001)	14.65	21.25

[a]Two rank truncation ratios N_μ/N_{vc} = 0.001, 0.01, and 0.1 are used in the LR-TDDFT + ISDF calculations.

for the C_{60} and Si_{64} systems are 2382.68 and 3238.45 s, respectively. We use three rank truncation ratios N_μ/N_{vc} of 0.001, 0.01, and 0.1 in the LR-TDDFT + ISDF calculations. We find that the ISDF decomposition can accelerate the direct LR-TDDFT calculations by a factor of 3 for both C_{60} and Si_{64} systems. Interestingly, the iterative Davidson method can further reduce the total time to 168.51 and 189.72 s for the C_{60} and Si_{64} systems, respectively. By combining the iterative Davidson method with ISDF decomposition in the LR-TDDFT calculations, we can significantly reduce the computational time to 14.65 (46.97) s and 21.25 (55.71) s with the rank truncation ratio of N_μ/N_{vc} = 0.001 (0.01) for the C_{60} and Si_{64} systems, respectively. Therefore, the Davidson + ISDF method can accelerate the LR-TDDFT calculations by nearly 2 orders of magnitude compared to conventional direct diagonalization calculations (explicitly constructing and directly diagonalizing the LR-TDDFT Hamiltonian).

In detail, we check the computational efficiency by using the ISDF decomposition to accelerate explicitly constructing and directly diagonalizing the LR-TDDFT Hamiltonian as shown in Table 4. For the Si_{64} system (N_r = 205379, N_g = 13133, and

Table 4. Computational Time (in s) Spent in the LR-TDDFT Calculations with the ISDF Decomposition To Reduce the Cost for Explicitly Constructing the Hartree V_H and Exchange-Correlation V_{xc} Integrals as well as Directly Diagonalizing the LR-TDDFT Hamiltonian H for the Si_{64} System

method	V_H	V_{xc}	diag H	total
direct	76.70	1203.44	1851.59	3238.45
ISDF (0.1)	1.21	23.82	1220.92	1532.87
ISDF (0.01)	0.027	0.778	1227.58	1347.09
ISDF (0.001)	0.003	0.058	1279.70	1283.78

$N_v = N_c$ = 128), the times spent in explicitly constructing the Hartree V_H and exchange-correlation V_{xc} integrals as well as directly diagonalizing the LR-TDDFT Hamiltonian H in the LR-TDDFT calculations are 194.13 (76.70 + 117.43), 1203.44, and 1851.59 s, respectively. Notice that the exchange-correlation integral V_{xc} is directly computed in real space but with a high computational cost of $N_rN_v^2N_c^2 \sim$ 1203.44 s, while the Hartree integral V_H is transformed and computed in reciprocal space with a small computational cost of $N_gN_v^2N_c^2 \sim$ 76.70 s, in which an extra cost of $N_gN_vN_c \log N_g \sim$ 117.43 s for the FFTs is required to transfer between real and reciprocal spaces. In particular, an ultrahigh computational cost of $N_v^3N_c^3 \sim$ 1851.59 s is spent for directly diagonalizing the LR-TDDFT Hamiltonian H. Therefore, the total time spent in the LR-TDDFT calculations for the Si_{64} system is as expansive as 3238.45 s.

As discussed in Section 2.3, the ISDF decomposition can significantly reduce the high computational cost for explicitly constructing the Hartree and exchange-correlation integrals to $N_gN_\mu^2 + N_rN_\mu^2 + N_\mu N_v^2N_c^2 \sim 0.037 + 0.058 + 0.381 = 0.476$ s under the ISDF ABFs (the rank truncation ratio N_μ/N_{vc} is set to 0.001 in this case and corresponding rank parameter $t = N_\mu/N_v$ = 0.128). Furthermore, the extra cost of FFTs is also significantly reduced and only required $N_gN_\mu \log N_g \sim 0.034$ s. Therefore, the computational cost of explicitly constructing the Hartree and exchange-correlation integrals under the ISDF ABFs is almost negligible in the LR-TDDFT calculations for the Si_{64} system. The total times of ISDF are 1.18 (0.91 + 0.27), 14.47 (11.86 + 2.60), and 270.04 (238.86 + 31.18) s for the rank truncation ratio N_μ/N_{vc} = 0.001, 0.01, and 0.1 used in the LR-TDDFT + ISDF calculations, respectively. It should be noticed that, for the case of the rank truncation ratio N_μ/N_{vc} = 0.1, the QRCP time (238.86 s) for selecting the interpolation points in ISDF becomes expensive. This issue can be solved by using the machine learning methods (K-means clustering),

https://dx.doi.org/10.1021/acs.jctc.9b01019
J. Chem. Theory Comput. 2020, 16, 964−973

which are much cheaper than QRCP but with similar computational accuracy.[31] However, direct diagonalization of LR-TDDFT Hamiltonian H still takes a high computational cost of 1279.70 s, and the total time is up to 1283.78 s.

This issue can be efficiently solved by using the iterative Davidson diagonalization method, which only computes a series of desired low excitation energies in the LR-TDDFT eigenvalue problem. The total time is further reduced to 189.72 s by using the iterative Davidson method in the LR-TDDFT calculations for the Si_{64} system as shown in Table 5. In detail, for the initialization at the beginning of Davidson iterations, it takes 6.44 s for computing the valence-conduction orbital products P_{vc} in real space.

Table 5. Computational Time (in s) Spent in the LR-TDDFT Calculations Combining the Iterative Davidson Method with ISDF Decomposition for the Si_{64} System, Including the Initialization at the Beginning of Davidson Iterations, the Computation of Projected Density $PS_k = P_{vc}S_k$, and Residual Vectors $R_k = HX_k - \Lambda_k X_k$, as well as the Diagonalization of Projected LR-TDDFT Hamiltonian H_s during Each Davidson Iteration[a]

method	init	PS_k	R_k	diag H_s	total
iterative	6.44	3.59	10.43	0.031	189.72
ISDF (0.1)	269.60	0.061	5.44	0.276	344.58
ISDF (0.01)	14.91	0.014	0.051	0.025	55.71
ISDF (0.001)	1.17	0.008	0.079	0.023	21.25

[a]The Davidson method requires 9 times of iterations for the Si_{64} system.

During each Davidson iteration, there are two expensive parts: one is to compute the projected density $PS_k = P_{vc}S_k$ with a computational cost of $kN_gN_vN_c \sim 3.59$ s, and another is to compute the residual vectors $R_k = HX_k - \Lambda_k X_k$ with a computational cost of $k(N_g + N_r)N_vN_c \sim 10.43$ s. In particular, the diagonalization part only takes 0.031 s, which is much faster than that (1851.59 s) in the direct diagonalization method. The Davidson method requires 9 times of iterations for the Si_{64} system, and its total time is about 189.72 s. Notice that other cheap parts during the Davidson iteration are not discussed in detail here.

Combining the iterative Davidson method with ISDF decomposition in the LR-TDDFT calculations, the computational cost of the Davision + ISDF method can be significantly reduced to $N_\mu N_v N_c$. In detail, the first step is to project the LR-TDDFT Hamiltonian H on the ISDF ABFs. The expensive part is the ISDF decomposition, which takes 1.17 (14.91 and 269.60) s when the the rank truncation ratio N_μ/N_{vc} is set to 0.001 (0.01 and 0.1) for the Si_{64} system. This part only takes one time as the initialization at the beginning of Davidson iterations for the Davision + ISDF method.

During each Davidson iteration in the ISDF + Davidson method, two expensive parts for computing the projected density and residual vectors only require a low computational cost of $N_\mu N_v N_c$ and the computational time is almost negligible, only takes 0.008 + 0.079 = 0.088 s. Therefore, the total time of the Davision + ISDF method only requires 21.25 s, which is much faster than that (189.72 s) used in the standard Davidson method.

3.3. Applications to Liquid Water on 2D Semiconductors. The ISDF method can significantly reduce the computational cost of excitation energies in the LR-TDDFT calculations and enable us to examine the excited-state properties of liquid water absorption on 2D semiconductors at the nanoscale. It is well known that, due to desirable optoelectronic properties (ideal band gap, high carrier mobility, and strong visible light absorption), 2D semiconductors,[41,42] such as graphitic carbon nitride (g-C_3N_4),[43] molybdenum disulfide (MoS_2),[44] and phosphorene,[45] have been proposed as potential candidates for photocatalytic water splitting in photoelectrochemical cells. Therefore, great efforts have been made to theoretically reveal the intrinsic mechanism of the photocatalytic water splitting process in 2D semiconductors, especially the energy band diagram of water and 2D semiconductors.[45] However, the excited-state properties of liquid water on 2D semiconductors at the nanoscale, known as the dielectric screening effect, are rarely examined due to the ultrahigh computational cost in the LR-TDDFT calculations.

In this work, we investigate the excited-state properties of liquid water absorption on MoS_2 and phosphorene by using the LR-TDDFT + ISDF calculations. We choose five systems, including liquid water $(H_2O)_{32}$ (N_o = 128), MoS_2 ($Mo_{12}S_{24}$, N_o = 108), and phosphorene (P_{24}, N_o = 60) monolayers as well as liquid water absorption on MoS_2 ($(H_2O)_{32}/Mo_{12}S_{24}$, N_o = 236) and phosphorene ($(H_2O)_{32}/P_{24}$, N_o = 188) as shown in Figure 4a,b. In particular, the atomic structures of liquid water

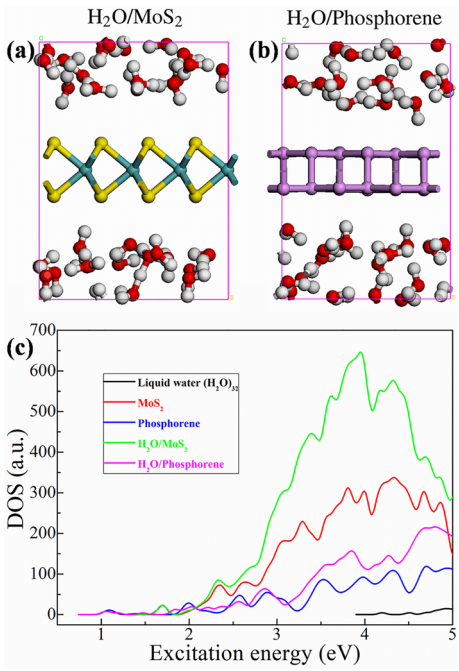

Figure 4. Side views of atomic structures of liquid water $(H_2O)_{32}$ absorption on 2D (a) MoS_2 and (b) phosphorene. The white, red, violet, yellow, and blue balls denote hydrogen, oxygen, phosphorus, sulfur, and molybdenum atoms, respectively. (c) Density of states (DOS) of excitation energies of liquid water, 2D MoS_2, and phosphorene monolayers as well as liquid water absorption on MoS_2 and phosphorene computed with the LR-TDDFT + ISDF calculations.

$(H_2O)_{32}$ are obtained starting from a prepared initial guess.[46] We set the kinetic energy cutoff to be 20 Ha for these five systems. We first perform the ab initio molecular dynamics (AIMD) simulations at room temperature (T = 300 K) for these five systems and then relax the geometry structures with a nonlinear conjugate gradient (CG) algorithm until total

https://dx.doi.org/10.1021/acs.jctc.9b01019
J. Chem. Theory Comput. 2020, 16, 964−973

energy and atomic forces are converged within error tolerances of 10^{-5} eV and 10^{-2} eV·Å^{-1}, respectively. We set the numbers of selected valence and conduction orbitals in the LR-TDDFT calculations to be $N_v = N_c = 60$ (the number of excitation energies is 3600) and the rank truncation ratio N_μ/N_{vc} to be 0.01 for the ISDF decomposition with a maximum relative error of 0.01 for these five systems.

We compute the density of states of excitation energies of liquid water, MoS_2, and phosphorene monolayers as well as liquid water absorption on MoS_2 and phosphorene by using the LR-TDDFT + ISDF calculations as shown in Figure 4c. The lowest excitation energies (first excitation energies) are 4.20, 1.7, and 1.1 eV for liquid water, MoS_2, and phosphorene, respectively. It should be noticed that the black curve of liquid water is much lower than those of other systems because the excitation energies of liquid water are much larger than those of other systems (Supporting Information). For liquid water absorption on MoS_2 and phosphorene, the lowest excitation energies are slightly changed to 1.7 and 1.1 eV, respectively. Furthermore, we find that the aqueous environment has a weak effect on low excitation energies (<2.0 eV) of 2D semiconductors for photocatalytic water splitting.

However, as the excitation energies become larger, such an aqueous effect becomes stronger after water adsorption on the photocatalysts due to the strong dielectric screening effect of water. Thus, the water environment has a strong effect on the high excitation energies (>2.5 eV) of 2D semiconductors for photocatalytic water splitting. In particular, for water absorption on MoS_2, the highest peak is transferred from 4.4 to 3.6 eV; thus, the water environment induces a red-shift for water absorption on MoS_2. Liquid water induces a significant increase of the excitation states above 2.4 eV for MoS_2 and 6.2 eV for phosphorene. Furthermore, for water absorption on MoS_2 and phosphorene, there are much more excited states between water and them. Therefore, the number of excited states of 2D semiconductors upon water absorption has increased a lot compared to freestanding cases. Therefore, the aqueous environment can efficiently enhance the excitation processes and generate more new excited states between water and 2D semiconductors during photocatalytic water splitting.

4. CONCLUSIONS AND OUTLOOK

In summary, we demonstrate that the interpolative separable density fitting (ISDF) decomposition combined with the iterative diagonalization method can be used to efficiently and accurately accelerate linear-response time-dependent density functional theory (LR-TDDFT) calculations in molecules and solids. The iterative ISDF method allows us to reduce the complexity of the Hamiltonian construction from $O(N_e^6)$ to $O(N_e^3)$ with a small pre-constant. We show that this method accurately reproduces excitation energies in the fullerene (C_{60}) molecule and bulk silicon Si_{64} system with significantly reduced computational cost compared to conventional direct and iterative calculations.

We also use the LR-TDDFT + ISDF calculations to investigate the excited-state properties of liquid water absorption on MoS_2 and phosphorene by using the LR-TDDFT calculations. Our computational results show that the water environment has a weak effect on low excitation energies but a strong effect on high excitation energies of 2D semiconductors during photocatalytic water splitting.

The performance results reported here are based on a sequential implementation of the ISDF method. In the near future, we will implement a parallel version suitable for large-scale distributed memory parallel computers. Such an implementation will allow us to tackle much larger problems for which the favorable scaling of the ISDF approach will be more pronounced.

■ ASSOCIATED CONTENT

Supporting Information

The Supporting Information is available free of charge at https://pubs.acs.org/doi/10.1021/acs.jctc.9b01019.

Computational scaling of the Davidson method for bulk silicon systems and the excitation energies of liquid water, MoS_2, phosphorene, and absorption systems (PDF)

■ AUTHOR INFORMATION

Corresponding Authors

Jie Liu − *University of Science and Technology of China, Hefei, China*; Email: liujie86@ustc.edu.cn

Jinlong Yang − *University of Science and Technology of China, Hefei, China*; orcid.org/0000-0002-5651-5340; Email: jlyang@ustc.edu.cn

Other Authors

Wei Hu − *University of Science and Technology of China, Hefei, China, and Lawrence Berkeley National Laboratory, Berkeley, California*; orcid.org/0000-0001-9629-2121

Yingzhou Li − *Duke University, Durham, North Carolina*; orcid.org/0000-0003-1852-3750

Zijing Ding − *University of Science and Technology of China, Hefei, China*

Chao Yang − *Lawrence Berkeley National Laboratory, Berkeley, California*

Complete contact information is available at: https://pubs.acs.org/10.1021/acs.jctc.9b01019

Notes

The authors declare no competing financial interest.

■ ACKNOWLEDGMENTS

This work is supported by National Natural Science Foundation of China (21688102, 21803064, 21803065, 21803066), by National Key Research and Development Program of China (2016YFA0200604), Anhui Initiative in Quantum Information Technologies (AHY090400), Strategic Priority Research Program of Chinese Academy of Sciences (XDC01040100), Research Start-Up Grants (KY2340000094) and Academic Leading Talents Training Program (KY2340000103) from the University of Science and Technology of China, and Chinese Academy of Sciences Pioneer Hundred Talents Program. This work is also partly supported by the U.S. Department of Energy, Office of Science, Office of Advanced Scientific Computing Research, Scientific Discovery through Advanced Computing (SciDAC) program. The authors thank USTC, CAS, Tianjin, and Shanghai Supercomputer Centers for the computational resources. The authors also thank the National Energy Research Scientific Computing (NERSC) Center for making computational resources available to them.

REFERENCES

(1) Runge, E.; Gross, E. K. U. Density-functional theory for time-dependent systems. *Phys. Rev. Lett.* **1984**, *52*, 997.

(2) Beck, T. L. Real-space mesh techniques in density-functional theory. *Rev. Mod. Phys.* **2000**, *72*, 1041.

(3) Onida, G.; Reining, L.; Rubio, A. Electronic excitations: density-functional versus many-body Green's-function approaches. *Rev. Mod. Phys.* **2002**, *74*, 601.

(4) Yabana, K.; Bertsch, G. F. Time-dependent local-density approximation in real time. *Phys. Rev. B* **1996**, *54*, 4484.

(5) Casida, M. E. Response Theory for Molecules. *Recent Advances in Density Functional Methods:(Part 1)*; World Scientific Publishing Co Pte Ltd, 1995, *1*, 155, 10.1142/9789812830586_0005.

(6) Sternheimer, R. M. Electronic Polarizabilities of Ions from the Hartree-Fock Wave Functions. *Phys. Rev.* **1954**, *96*, 951.

(7) Davidson, E. R. The iterative calculation of a few of the lowest eigenvalues and corresponding eigenvectors of large real-symmetric matrices. *J. Comput. Phys.* **1975**, *17*, 87−94.

(8) Lanczos, C. *Applied analysis*; Dover: New York, 1988.

(9) Knyazev, A. V. Toward the Optimal Preconditioned Eigensolver: Locally Optimal Block Preconditioned Conjugate Gradient Method. *SIAM J. Sci. Comput.* **2001**, *23*, 517−541.

(10) Malcoğlu, O. B.; Gebauer, R.; Rocca, D.; Baroni, S. turboTDDFT - A code for the simulation of molecular spectra using the LiouvilleLanczos approach to time-dependent density-functional perturbation theory. *Comput. Phys. Commun.* **2011**, *182*, 1744−1754.

(11) Ge, X.; Binnie, S. J.; Rocca, D.; Gebauer, R.; Baroni, S. turboTDDFT 2.0 - Hybrid functionals and new algorithms within time-dependent density-functional perturbation theory. *Comput. Phys. Commun.* **2014**, *185*, 2080−2089.

(12) Früchtl, H. A.; Kendall, R. A.; Harrison, R. J.; Dyall, K. G. An implementation of RISCF on parallel computers. *Int. J. Quantum Chem.* **1997**, *64*, 63−69.

(13) Weigend, F. A fully direct RI-HF algorithm: Implementation, optimised auxiliary basis sets, demonstration of accuracy and efficiency. *Phys. Chem. Chem. Phys.* **2002**, *4*, 4285−4291.

(14) Aquilante, F.; Pedersen, T. B.; Lindh, R. Low-cost evaluation of the exchange Fock matrix from Cholesky and density fitting representations of the electron repulsion integrals. *J. Chem. Phys.* **2007**, *126*, 194106.

(15) Ren, X.; Rinke, P.; Blum, V.; Wieferink, J.; Tkatchenko, A.; Sanfilippo, A.; Reuter, K.; Scheffler, M. Resolution-of-identity approach to Hartree−Fock, hybrid density functionals, RPA, MP2 and GW with numeric atom-centered orbital basis functions. *New J. Phys.* **2012**, *14*, No. 053020.

(16) Merlot, P.; Kjærgaard, T.; Helgaker, T.; Lindh, R.; Aquilante, F.; Reine, S.; Pedersen, T. B. Attractive electronelectron interactions within robust local fitting approximations. *J. Comput. Chem.* **2013**, *34*, 1486−1496.

(17) Manzer, S.; Horn, P. R.; Mardirossian, N.; Head-Gordon, M. Fast, accurate evaluation of exact exchange: The occ-RI-K algorithm. *J. Chem. Phys.* **2015**, *143*, No. 024113.

(18) Neese, F.; Wennmohs, F.; Hansen, A.; Becker, U. Efficient, approximate and parallel HartreeFock and hybrid DFT calculations. A 'chain-of-spheres' algorithm for the HartreeFock exchange. *Chem. Phys.* **2009**, *356*, 98−109.

(19) Izsák, R.; Neese, F. An overlap fitted chain of spheres exchange method. *J. Chem. Phys.* **2011**, *135*, 144105.

(20) Guidon, M.; Hutter, J.; Vandevondele, J. Auxiliary density matrix methods for hartree-fock exchange calculations. *J. Chem. Theory Comput.* **2010**, *6*, 2348−2364.

(21) Merlot, P.; Izsák, R.; Borgoo, A.; Kjærgaard, T.; Helgaker, T.; Reine, S. Charge-constrained auxiliary-density-matrix methods for the Hartree−Fock exchange contribution. *J. Chem. Phys.* **2014**, *141*, No. 094104.

(22) Parrish, R. M.; Hohenstein, E. G.; Martínez, T. J.; Sherrill, C. D. Tensor hypercontraction. II. Least-squares renormalization. *J. Chem. Phys.* **2012**, *137*, 224106.

(23) Parrish, R. M.; Hohenstein, E. G.; Martínez, T. J.; Sherrill, C. D. Discrete variable representation in electronic structure theory: Quadrature grids for least-squares tensor hypercontraction. *J. Chem. Phys.* **2013**, *138*, 194107.

(24) Rappoport, D.; Furche, F. Analytical time-dependent density functional derivative methods within the RI-J approximation, an approach to excited states of large molecules. *J. Chem. Phys.* **2005**, *122*, No. 064105.

(25) Goedecker, S.; Teter, M.; Hutter, J. Separable Dual-Space Gaussian Pseudopotentials. *Phys. Rev. B* **1996**, *54*, 1703.

(26) Perdew, J. P.; Burke, K.; Ernzerhof, M. Generalized Gradient Approximation Made Simple. *Phys. Rev. Lett.* **1996**, *77*, 3865.

(27) Lu, J.; Ying, L. Compression of the Electron Repulsion Integral Tensor in Tensor Hypercontraction Format with Cubic Scaling Cost. *J. Comput. Phys.* **2015**, *302*, 329−335.

(28) Lu, J.; Thicke, K. Cubic scaling algorithms for RPA correlation using interpolative separable density fitting. *J. Comput. Phys.* **2017**, *351*, 187−202.

(29) Lin, L.; Xu, Z.; Ying, L. Adaptively Compressed Polarizability Operator for Accelerating Large Scale Ab Initio Phonon Calculations. *Multiscale Model. Simul.* **2017**, *15*, 29−55.

(30) Hu, W.; Lin, L.; Yang, C. Interpolative Separable Density Fitting Decomposition for Accelerating Hybrid Density Functional Calculations with Applications to Defects in Silicon. *J. Chem. Theory Comput.* **2017**, *13*, 5420−5431.

(31) Dong, K.; Hu, W.; Lin, L. Interpolative Separable Density Fitting through Centroidal Voronoi Tessellation with Applications to Hybrid Functional Electronic Structure Calculations. *J. Chem. Theory Comput.* **2018**, *14*, 1311−1320.

(32) Hu, W.; Lin, L.; Yang, C. Projected Commutator DIIS Method for Accelerating Hybrid Functional Electronic Structure Calculations. *J. Chem. Theory Comput.* **2017**, *13*, 5458−5467.

(33) Hu, W.; Shao, M.; Cepellotti, A.; da Jornada, F. H.; Lin, L.; Thicke, K.; Yang, C.; Louie, S. G. *Lecture Notes in Computer Science*; Springer International Publishing, 2018, pp 604−617.

(34) Malone, F. D.; Zhang, S.; Morales, M. A. Overcoming the Memory Bottleneck in Auxiliary Field Quantum Monte Carlo Simulations with Interpolative Separable Density Fitting. *J. Chem. Theory Comput.* **2019**, *15*, 256−264.

(35) Lee, J.; Lin, L.; Head-Gordon, M. Systematically Improvable Tensor Hypercontraction: Interpolative Separable Density-Fitting for Molecules Applied to Exact Exchange, Second- and Third-Order Møller-Plesset Perturbation Theory. *J. Chem. Theory Comput.* **2019**, 10.1021/acs.jctc.9b00820.

(36) Yang, C.; Meza, J. C.; Lee, B.; Wang, L.-W. KSSOLV a MATLAB toolbox for solving the KohnSham equations. *ACM Trans. Math. Software* **2009**, *36*, 1−35.

(37) Khatri, C. G.; Rao, C. R. Solutions to some functional equations and their applications to characterization of probability distributions. *Sankhya* **1968**, *30*, 167−180.

(38) Golub, G. H.; Reinsch, C. Singular Value Decomposition and Least Squares Solutions. *Numer. Math.* **1970**, *14*, 403−420.

(39) Hartwigsen, C.; Goedecker, S.; Hutter, J. Relativistic Separable Dual-Space Gaussian Pseudopotentials from H to Rn. *Phys. Rev. B* **1998**, *58*, 3641.

(40) Giannozzi, P.; Baroni, S.; Bonini, N.; Calandra, M.; Car, R.; Cavazzoni, C.; Ceresoli, D.; Chiarotti, G. L.; Cococcioni, M.; Dabo, I.; Corso, A. D.; de Gironcoli, S.; Fabris, S.; Fratesi, G.; Gebauer, R.; Gerstmann, U.; Gougoussis, C.; Kokalj, A.; Lazzeri, M.; Martin-Samos, L.; Marzari, N.; Mauri, F.; Mazzarello, R.; Paolini, S.; Pasquarello, A.; Paulatto, L.; Sbraccia, C.; Scandolo, S.; Sclauzero, G.; Seitsonen, A. P.; Smogunov, A.; Umari, P.; Wentzcovitch, R. M. QUANTUM ESPRESSO: A Modular and Open-Source Software Project for Quantum Simulations of Materials. *J. Phys.: Condens. Matter* **2009**, *21*, 395502.

(41) Osada, M.; Sasaki, T. Two-Dimensional Dielectric Nanosheets: Novel Nanoelectronics from Nanocrystal Building Blocks. *Adv. Mater.* **2012**, *24*, 210.

https://dx.doi.org/10.1021/acs.jctc.9b01019
J. Chem. Theory Comput. 2020, 16, 964−973

(42) Xu, M.; Liang, T.; Shi, M.; Chen, H. Graphene-Like Two-Dimensional Materials. *Chem. Rev.* **2013**, *113*, 3766.
(43) Wang, X.; Maeda, K.; Thomas, A.; Takanabe, K.; Xin, G.; Carlsson, J. M.; Domen, K.; Antonietti, M. A Metal-Free Polymeric Photocatalyst for Hydrogen Production from Water under Visible Light. *Nat. Mater.* **2009**, *8*, 76−80.
(44) Hinnemann, B.; Moses, P. G.; Bonde, J.; Jørgensen, K. P.; Nielsen, J. H.; Horch, S.; Chorkendorff, I.; Nørskov, J. K. Biomimetic hydrogen evolution: MoS2 nanoparticles as catalyst for hydrogen evolution. *J. Am. Chem. Soc.* **2005**, *127*, 5308−5309.
(45) Hu, W.; Lin, L.; Zhang, R.; Yang, C.; Yang, J. Highly Efficient Photocatalytic Water Splitting over Edge-Modified Phosphorene Nanoribbons. *J. Am. Chem. Soc.* **2017**, *139*, 15429−15436.
(46) DiStasio, R. A., Jr.; Santra, B.; Li, Z.; Wu, X.; Car, R. The individual and collective effects of exact exchange and dispersion interactions on the ab initio structure of liquid water. *J. Chem. Phys.* **2014**, *141*, No. 084502.

https://dx.doi.org/10.1021/acs.jctc.9b01019
J. Chem. Theory Comput. 2020, 16, 964−973